Fermi Edge Polaritons in a Microcavity Containing a High Density Two-Dimensional Electron Gas

A. Gabbay, Yulia Preezant, E. Cohen, and B. M. Ashkinadze
Solid State Institute, Technion-Israel Institute of Technology, Haifa 32000, Israel

L. N. Pfeiffer
Bell Laboratories, Alcatel-Lucent Technologies, Murray Hill, New Jersey 07974, USA
(Received 16 June 2006; published 10 October 2007)

Sharp, near band gap lines are observed in the reflection and photoluminescence spectra of GaAs/AlGaAs structures consisting of a modulation doped quantum well (MDQW) that contains a high density two-dimensional electron gas (2DEG) and is embedded in a microcavity (MC). The energy dependence of these lines on the MC-confined photon energy shows level anticrossings and Rabi splittings very similar to those observed in systems of undoped QW's embedded in a MC. The spectra are analyzed by calculating the optical susceptibility of the MDQW in the near band gap spectral range and using it within the transfer matrix method. The calculated reflection spectra indicate that the sharp spectral lines are due to $k_{\|} = 0$ cavity polaritons that are composed of *e-h* pair excitations just above the 2DEG Fermi edge and are strongly coupled to the MC-confined photons.

DOI: 10.1103/PhysRevLett.99.157402 PACS numbers: 78.67.De, 71.36.+c, 73.21.Fg

Cavity polaritons are the composite elementary excitations that arise from the strong interaction between confined photons in a microcavity (MC) and confined excitons in a semiconductor quantum well (QW) that is embedded in the MC [1,2]. The precondition for polariton formation is that the coupling strength between the exciton (energy E_X) and the MC photon (energy E_C) is larger than both exciton and confined photon linewidths [3,4]. This condition is easily met in high quality, undoped QW/MC structures, where the most prominent feature of the polariton energy dependence on E_C is level anticrossing in the resonance spectral range ($E_C \sim E_X$). The "level anticrossing diagram", extracted from transmission, reflection, and photoluminescence (PL) spectra, is commonly analyzed by using the coupled oscillators model [1,3]. This yields the Rabi splittings which measure the coupling strength of each exciton to the MC photon [1]. In GaAs/AlGaAs QW/MC's, at low temperatures, when only exciton-acoustic phonon scattering is effective, the observed polariton linewidths are 10–50 times smaller than their Rabi splitting [5]. Experiments show that polariton formation is greatly hindered by the presence of a photoexcited electron-hole (*e-h*) plasma in InGaAs/GaAs QW/MC's [6] or a photoexcited two-dimensional electron gas (2DEG) in GaAs/AlGaAs QW/MC's [7–9]. When the photoexcited electron density reaches the range of $n_e \sim 5 \times 10^{10}$ cm^{-2}, and the electrons are in close proximity to the excitons, then the exciton-MC photon system transforms into the weak coupling regime and the Rabi splittings are washed out. This was explained by tracing back the effects of a high n_e on excitons in bare QW's: (1) a large increase in the exciton linewidth is caused by efficient exciton-electron scattering [3,7]. (2) The exciton binding energy is reduced due to both phase space filling and screening of the *e-h* Coulomb interaction [10–12].

The present study demonstrates that a strong coupling is maintained between *e-h* pair excitations at the 2DEG Fermi edge and resonant MC photons, in GaAs/AlGaAs MC's with an embedded, modulation doped quantum well (MDQW). The experimental evidence is found in the observation of sharp, near band gap lines in the reflection and PL spectra, whose energy dependence on E_C shows level anticrossings and Rabi splittings that are similar to those of polaritons in undoped QW/MC's [1,2]. These polaritons are observed in MDQW-MC's having a 2DEG density as high as $n_e \sim 2 \times 10^{11}$ cm^{-2}, and where the doping layers are spaced far from the 2DEG. The experimental results are analyzed by applying the coupled oscillators model [1,3] and by calculating the reflection spectra (for a wide range of E_C values) using the optical susceptibility function model [13]. These model calculations show that the polaritons are formed of *e-h* pair excitations involving electron and hole states with in-plane wave vectors around the Fermi edge: $k_{\|e} = k_{\|h} \sim k_F$. The coherence between these *e-h* pair excitations, that is required for polariton formation, stems from the strong interaction of each *e-h* pair excitation with the same MC photon. This mechanism substitutes for the *e-h* Coulomb interaction that coherently couples *e-h* pair excitations near $k_{\|} = 0$ into bound excitons in undoped QW's. The experimental part consists of a comparative spectroscopic study of 200 Å wide $GaAs/Al_{0.1}Ga_{0.9}As$ MDQW's in two types of structures: (1) Single, bare MDQW's and (2) MDQW's that are embedded in either a λ or a 2λ wide $GaAs/Al_{0.1}Ga_{0.9}As$ MC (at the central antinode of the MC photon electric field). The cavity layer is cladded with $AlAs/Al_{0.1}Ga_{0.9}As$ distributed Bragg reflectors (15/25 periods). All the studied structures were grown by molecular beam epitaxy on (001)-oriented GaAs substrates. Two Si-doped layers were grown symmetrically on each side of the quantum well (QW), at exactly the same spacer layer width (500–1000 Å, depending on n_e). The range of 2DEG densities in the studied pairs of bare MDQW and MDQW-MC structures was $n_e = [(0.7 - 1.8) \pm 0.1] \times 10^{11}$ cm^{-2}. They all show similar spectroscopic results. In this Letter we report on the study of the MDQW embedded in a 2λ MC and the bare MDQW, both having $n_e = (1.0 \pm 0.1) \times 10^{11}$ cm^{-2}. The samples were immersed in liquid helium and illuminated with a tungsten filament lamp and with a Ti:sapphire laser. Both incoming and outgoing beams were aligned along the normal direction to the MC plane and were focused at the same point on the MC sample surface. In this way the polariton in-plane wave vector was defined within the range of $|\Delta k_{\|}| < 1 \times 10^4$ cm^{-1}. Figure 1 compares the $T = 2$ K reflection and PL spectra of a bare MDQW with those of a MDQW-MC, both having $n_e = (1 \pm 0.1) \times 10^{11}$ cm^{-2}. The reflection spectrum of the former [Fig. 1(a)] shows only two small and broad features that are due to the 2DEG ($\Delta R \sim 0.02$). The lower energy one is at the Fermi edge, $E_F = 1.525$ eV, where the PL spectrum cuts off. Figure 1(b) presents a series of reflection and PL spectra, measured at consecutive illumination points on the MDQW-MC sample surface. It is seen that the MC photon is tuned into resonance with two interband transitions of the MDQW (marked X_1 and X_2), thus forming three polariton lines. The peak energies of the reflection lines as a function of the detuning energy, $\delta = E_C - E_{X1}$, are plotted in Fig. 2. The extrapolated energies are $E_{X1} = 1.523$ eV and $E_{X2} = 1.526$ eV. In the resonance spectral range, $\delta \sim 0$, the largest reflection depth is observed, $\Delta R \sim 0.6$, and the smallest linewidths are 0.7, 1.0, and 2.8 $\pm$ 0.1 meV (corresponding to the lines in ascending energy order). The PL spectra were excited with a laser energy $E_L = 1.60$ eV and weak intensity. The PL is strongest for $\delta \sim 0$, and for $\delta < 0$ it is observed only at the MC photon line.

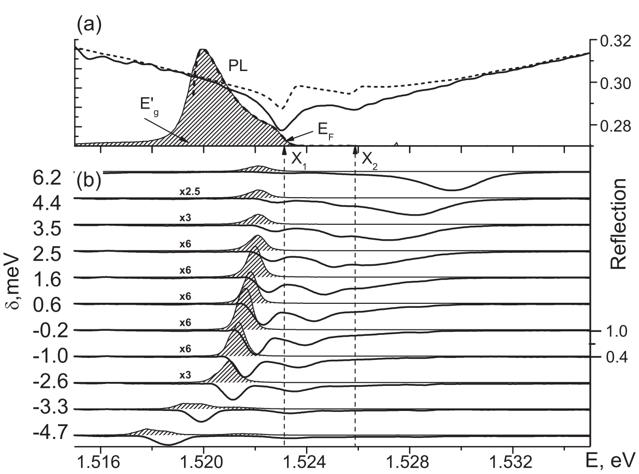

FIG. 1. Reflection (solid lines) and PL (shaded areas) spectra (at $T = 2$ K) of 200 Å wide MDQW structures containing a 2DEG with $n_e = (1 \pm 0.1) \times 10^{11}$ cm^{-2}. (a) Bare MDQW. (b) MDQW embedded in a 2λ wide MC. The reflection scale of all spectra was determined by normalization with respect to that of the MC Bragg reflectors. The spectra in (a) are shifted by -2 meV in order to have $E_F = E_{X1}$. This difference is due to small variations in QW width across the bare MDQW area. In (a), the broad reflection band is due to a short period superlattice grown on the thick GaAs buffer layer. The calculated reflection and PL spectra are shown by dotted and dashed lines, respectively. In (b), the spectra are shown for various detuning energies ($\delta = E_C - E_{X1}$). The multiplying factors refer only to the PL intensity (strongest for $\delta = 0$).

The level anticrossings seen in Fig. 2 are qualitatively similar to those observed in undoped GaAs/AlGaAs QW/MC's. Therefore, as a first stage in the analysis, the coupled oscillators model is applied to the polariton energy dependence on δ [1,2]. This model fitting yields the coupling strengths of X_1 and X_2 to the MC photon: $\Gamma_{X1} = 1.1 \pm 0.1$ meV and $\Gamma_{X2} = 0.8 \pm 0.1$ meV. The accuracy of the coupled oscillators model fitting of the polariton energies suggests that X_1 and X_2 are excitonlike transitions. However, no excitons are observed in the spectra of bare MDQW's with identical n_e, in concurrence with theory [10–12]. In order to further prove that X_1 and X_2 are not exciton lines, circularly polarized reflection and PL spectra were measured under a perpendicularly applied magnetic field ($B \leq 6.2$ T), for various δ values. Figure 3 shows representative data: it compares the reflection line energies measured (in σ^+ polarization) of the MDQW-MC, at $\delta = -2.8$ meV, with those of the bare MDQW. The observed fan diagrams are typical of interband transitions between the e and h Landau levels ($LL = 0$, 1 and 2) in QW's containing a 2DEG. The $LL = 0$ line has a nearly identical slope in both systems. The slope change at filling factor $\nu = 2$ [14] is used to determined the 2DEG density.

We thus propose that X_1 and X_2 are due to e-h pair excitations that couple strongly to the MC photon. In order

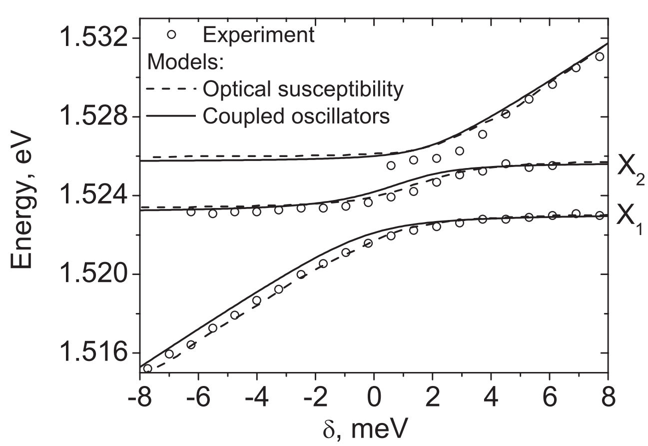

FIG. 2. The dependence of the peak polariton energy on detuning energy, $\delta = E_C - E_{X1}$ (level anticrossing diagram). The experimental points were measured from reflection spectra such as those shown in Fig. 1(b).

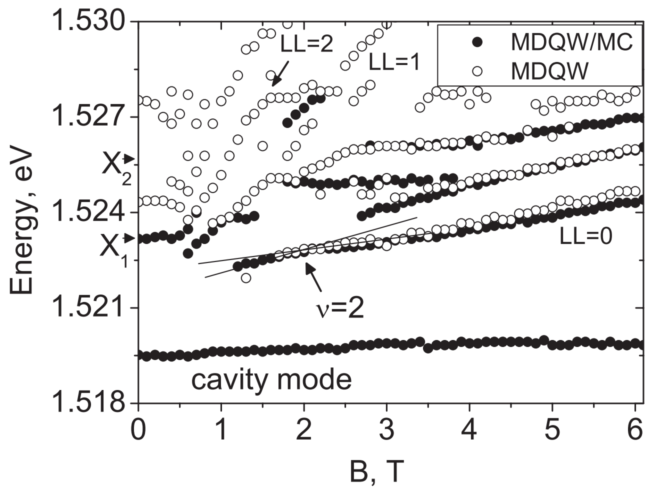

FIG. 3. Comparison between the energy dependence on perpendicularly applied magnetic field of the interband Landau transitions in the bare MDQW and the MDQW-MC systems (observed by reflection in σ^+ polarization). In the MDQW-MC, the detuning energy is $\delta = -2.8$ meV. The 2DEG density ($n_e = 1 \pm 0.1 \times 10^{11}$ cm^{-2}) is determined by the magnetic field at the $LL = 0$ line slope change (filling factor $\nu = 2$, as shown by the thin lines). The energies of the bare MDQW are shifted by -0.5 meV in order to have them coincide with those of the MDQW-MC.

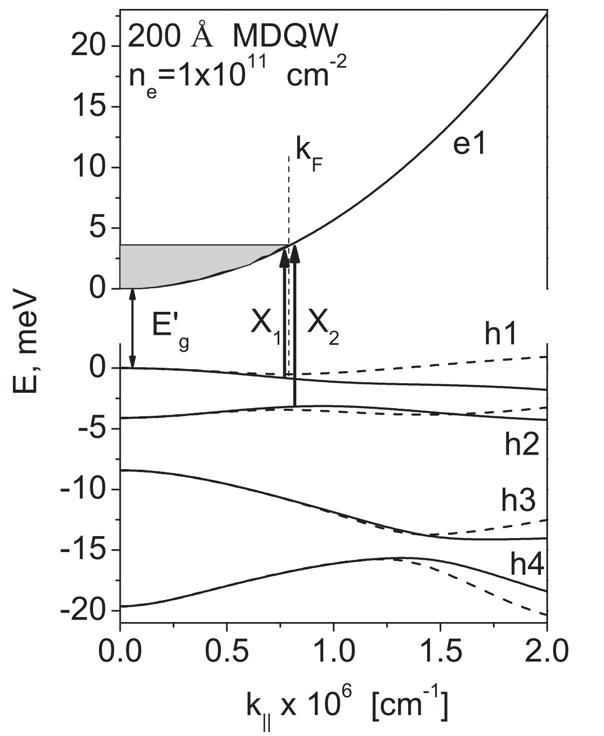

FIG. 4. Calculated dispersion curves of the lowest conduction subband ($e1$) and four highest valence subbands ($h1$-$h4$). The in-plane anisotropy of the valence subbands is demonstrated by the dispersion curves along the (010) and (110) directions (solid and dashed lines, respectively).

to examine this proposition we first calculate the in-plane dispersion of the conduction and valence subbands of a bare MDQW, incorporating the effect of the 2DEG Coulomb potential on both electrons and holes (Hartree approximation). Figure 4 shows the dispersion curves of the lowest conduction subband $e1$ and the top four valence subbands (denoted $h1$-$h4$), calculated for $n_e = 1 \times 10^{11}$ cm^{-2}. The accuracy of the calculated dispersion curves is examined by numerically calculating the PL spectral shape. This is done by summing over all the vertical $e1$-$h1$ transitions having energy of $E(\mathbf{k}_\parallel) = E'_g + E_{e1}(\mathbf{k}_\parallel) - E_{h1}(\mathbf{k}_\parallel)$, and the PL intensity is given by: $I_{\rm PL}(E) \propto \int d\mathbf{k}_\parallel f_c(E_{e1}(\mathbf{k}_\parallel), n_e)(1 - f_v(E_{h1}(\mathbf{k}_\parallel), n_e)) \times \delta(E - E(\mathbf{k}_\parallel))$. The Fermi distribution functions, f_c and f_v, are computed with $T = 2$ K. The calculated $I_{\rm PL}$ [dashed curve in Fig. 1(a)] fits well the experimental spectrum. The dispersion curves allow us to identify X_1 and X_2 as, respectively, $e1$-$h1$ and $e1$-$h2$ pair excitations, with $k_{\parallel e} = k_{\parallel h} \sim k_F$ (vertical arrows in Fig. 4). The calculated splitting between $e1$-$h1$ and $e1$-$h2$ at k_F (2.7 meV) agrees well with the measured value of $E_{X2} - E_{X1} = 2.6 \pm 0.1$ meV. The cavity polaritons that are composed of the $e1$-$h1$ and $e1$-$h2$ pair excitations have an in-plane wave vector $k_\parallel = 0$, since they are observed in normal incidence configuration. In the second stage of the model we study the response of these pair excitations to light in the near band gap spectral range by calculating their contribution to the MDQW optical susceptibility function [13]:

$$\chi_e(E) = \sum_{\mathbf{k}_\parallel, i} \frac{|d_{e1,hi}(\mathbf{k}_\parallel)|^2}{SL_{\rm QW}} [f_c(E_{e1}(\mathbf{k}_\parallel)) - f_v(E_{hi}(\mathbf{k}_\parallel))] \times \left[\frac{1}{(E_{hi}(\mathbf{k}_\parallel) - E_{e1}(\mathbf{k}_\parallel) + E + i\gamma)} - \frac{1}{(E_{e1}(\mathbf{k}_\parallel) - E_{hi}(\mathbf{k}_\parallel) + E + i\gamma)} \right]. \quad (1)$$

The transition dipoles $d_{e1,hi}$ ($i = 1, 2$) are chosen to have a $k_\parallel$-independent term plus a term that simulates an enhancement near k_F: $d_{e1,hi}(k_\parallel) = a_i + b_i \exp\{-\frac{(k_\parallel - k_F)^2}{\sigma_1^2}\}$. The electron dephasing rate is taken as: $\gamma(k_\parallel) = \gamma_0(1 - \exp\{-\frac{(k_\parallel - k_F)^2}{\sigma_2^2}\})\Theta(k_\parallel - k_F) + \gamma_{\rm min}$, where $\Theta(x)$ is the step function. The total MDQW optical susceptibility function is given by $\chi = \chi_{\rm GaAs} + \chi_e$. From it, the refraction index is calculated: $n(E) = {\rm Re}\,(n) + {\rm Im}\,(n) = (1 + 4\pi\chi)^{1/2}$ and is shown in Fig. 5(a). The parameter values used in the calculation (for $n_e = 1 \times 10^{11}$ cm^{-2}) are $b_{e1,h1} = 4.6 \times 10^{-29}$ C · m, which corresponds to $(E_p)_{e1,h1} = 2m_0(d_{e1,h1}E_g/\hbar e)^2 \approx 5$ eV; $\sigma_{1,h1} = 10^5$ cm^{-1}, corresponding to ≈ 0.9 meV; $b_{e1,h2} = b_{e1,h1}/\sqrt{2}$ and $\sigma_{1,h2} = 5 \times 10^5$ cm^{-1}, corresponding to $\approx$ 4.5 meV. The $k_\parallel$-independent terms are $a_{e1,h1} = \sqrt{2}a_{e1,h2} = b_{e1,h1}/14$. The electron dephasing term has $\gamma_0 = 5$ meV, $\gamma_{\rm min} = 50$ μeV, and $\sigma_2 = \sigma_1$. In the final

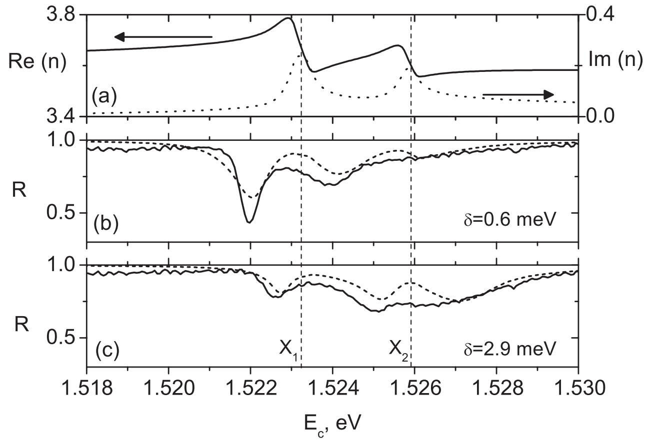

FIG. 5. (a) The refraction index dependence on energy, $n(E)$, calculated for a MDQW with $n_e = 1 \times 10^{11}$, using Eq. (1) and the parameters as given in the text. (b) The reflection spectrum of the MDQW-MC observed near resonance with X_1 (solid line) and the spectrum calculated using the transfer matrix method and $n(E)$ calculated by using Eq. (1) (dashed line). (c) Same as (b) but near resonance with X_2.

stage of the model we calculate the polariton reflection spectrum using the transfer matrix method [1–3] with the calculated $n(E)$ [Fig. 5(a)] introduced into the transfer matrix of the QW. Figures 5(b) and 5(c) show two examples of the reflection spectra calculated near resonance with X_1 and X_2 (dashed lines), compared with the corresponding experimental spectra (solid lines). The parameter values of $d_{e1,hi}$ and γ were varied to best fit the experimental polariton energies and intensities in the resonance spectral range. The calculated reflection spectra are most sensitive to the strength and width of the transition dipoles. Using the same parameters (quoted above), the reflection spectra were then calculated for a series of E_C values in the range of 1.50–1.56 eV. The energies of the three polariton lines were extracted from them and are shown in Fig. 2 (dashed lines). The resulting level anticrossing diagram fits the experimental polariton energy dependence on E_C with the same accuracy as that of the coupled oscillators model. This proves that the model based on the optical susceptibility of noninteracting *e-h* pair excitations explains well the origin of the observed polaritons. Furthermore, we calculated the reflection spectrum of the bare MDQW [dotted line in Fig. 1(a)]. In order to fit the experimental spectrum, the values of $d_{e1,h1}$ and of $d_{e1,h2}$ had to be reduced by factors of $\sqrt{2}$ and 2, respectively.

We summarize this study by pointing out several conclusions that are drawn from the above analysis: (1) the cavity polaritons observed in MDQW-MC's that contain a 2DEG with densities that preclude bound excitons are formed by the strong coupling between noninteracting *e-h* pair excitations just above the 2DEG Fermi edge and the MC-confined photons. (2) The transition dipoles that are introduced into χ_e increase the coupling strength. Since the *e-h* Coulomb interaction is screened, the $k_{\|}$-dependent term in the transition dipoles (peaked near k_F) simulates the coherence that is established between all the pair excitations having the same energy by their coupling to the same MC photon. (3) In comparing the polariton reflection spectra of the MDQW-MC with those of the bare MDQW, larger transition dipole strengths are obtained in fitting the calculated polariton spectra than in the bare MDQW case. This is an additional demonstration of the coherence between the *e-h* pair excitations that is induced by their interaction with the MC photon. We note that a related effect was theoretically studied in the case of undoped QW/MC's where the exciton-MC photon coupling is much stronger than the *e-h* Coulomb interaction. All the bound and continuum exciton states are then admixed by the strong coupling and the polariton line shapes are greatly distorted [15]. In the present case of noninteracting *e-h* pairs, their strong coupling with the MC photon substitutes for exciton coherence in undoped QW/MC's. In this respect, the polaritons in MDQW-MC are fundamentally different from those commonly observed in undoped QW/MC. (4) Finally we note that in MDQW structures, dephasing of the *e-h* pair excitations by charged donors in the remote doping layers is slow. This distinguishes the MDQW-MC system from intensely photoexcited QW/MC systems [7–9], where unbound electron-hole scattering leads to fast dephasing and disappearance of the polaritons.

The research at the Technion was done in the Barbara and Norman Seiden Center for Advanced Optoelectronics and was supported by the Israel-US Binational Science Foundation (BSF), Jerusalem.

[1] Y. Yamamoto *et al.*, *Semiconductor Cavity Quantum Electrodynamics*, Springer Tracts in Modern Physics Vol. 169 (Springer, New York, 2000).
[2] M. S. Skolnick *et al.*, Semicond. Sci. Technol. **13**, 645 (1998).
[3] G. Khitrova *et al.*, Rev. Mod. Phys. **71**, 1591 (1999).
[4] V. Savona *et al.*, Solid State Commun. **93**, 733 (1995).
[5] J. R. Jensen *et al.*, Appl. Phys. Lett. **76**, 3262 (2000).
[6] R. Houdrè *et al.*, Phys. Rev. B **52**, 7810 (1995).
[7] G. Ramon *et al.*, Phys. Rev. B **65**, 085323 (2002).
[8] A. Qarry *et al.*, Semicond. Sci. Technol. **18**, S331 (2003).
[9] M. Perrin *et al.*, Phys. Rev. B **72**, 075340 (2005).
[10] D. A. Kleinman, Phys. Rev. B **32**, 3766 (1985).
[11] F. G. Pikus, Sov. Phys. Semicond. **26**, 26 (1992).
[12] D. V. Kulakovskii *et al.*, JETP Lett. **74**, 118 (2001).
[13] H. Haug and S. W. Koch, *Quantum Theory of the Optical and Electronic Properties of Semiconductors* (World Scientific, Singapore, 1990).
[14] K.-B. Broocks, Phys. Rev. B **66**, 041309 (2002).
[15] D. S. Citrin *et al.*, Phys. Rev. B **68**, 205325 (2003).